

THE NORMAL STATE HALL EFFECT IN NdBa_{2-x}La_xCu₃O_{7-δ}: EVIDENCE FOR HOLE LOCALIZATION BY LA DOPING

S. R. GHORBANI* and F. ABRINAEY

*Department of Physics, Tarbiat Moallem University of Sabzevar,
P.O. Box 397, Sabzevar, Iran
ghorbani@sttu.ac.ir

Received 16 July 2008

The transport properties of sintered samples of NdBa_{2-x}La_xCu₃O_{7-δ} with $0 \leq x \leq 0.3$ have been studied in the normal state by Hall effect measurements. The Hall coefficient, R_H is positive in the normal state and increases with increasing La doping concentration over the whole temperature range from the critical temperature, T_c , up to room temperature. The results for the Hall coefficient as a function of temperature and doping concentration were analyzed within the phenomenological narrow band and Anderson models. A good agreement between models and data was obtained. As in the phenomenological narrow band model, the band widths increase with increasing doping concentration. As in the Anderson model, the Hall angle is proportional to T^2 over the whole measured temperature range for all samples. The obtained results for both models supported the view that La doping introduces electronic disorder into the CuO₂ planes. The tendency towards localization is driven by electronic disorder. In addition to hole filling, the localization is another reason for the decreasing superconducting critical temperature in these samples.

Keywords: Superconductivity; localization; Hall coefficient.

1. Introduction

The phenomenon of superconductivity is one of main interests of physics research in the current century, but there are still major questions about its mechanisms. The measurement of the transport properties, such as resistivity, thermoelectric power, and Hall effect in the normal state give us outstanding information to use in the elucidation of the phenomenon of superconductivity in cuprates. The Hall coefficient, R_H , shows a drastic temperature dependence at low temperatures, while at high temperatures (~ 1000 K), it is nearly constant. R_H has a temperature dependence of approximately $1/T$ over a quite wide range of temperatures. $dR_H/dT < 0$ is observed in the hole-doped compounds while $dR_H/dT > 0$ is realized in the electron-doped compounds. In the underdoped compounds and at low temperatures, $|R_H| \gg |1/ne|$.¹

The doping effects in cuprates have led to expanded research in this field.² The superconductivity and electronic properties are highly sensitive to doping in the $\text{NdBa}_{2-x}\text{La}_x\text{Cu}_3\text{O}_{7-\delta}$. This is because doping in these compounds strongly affects the carriers density and structural properties by introducing non-isovalent disorder. The light atoms, such as La, with largest ionic radius in the rare earth group, have a greater tendency to occupy Ba sites. It was found that among the two and three valent elements, only Sr^{+2} and La^{+3} enter the Ba sites in the 123 structure.³

There have been a large number of theories to explain the behavior of the cuprate high temperature superconductors. So far, however, there has been no agreement on one particular theory, since all aspects are not completely explained by any of the theories. Several models have been proposed to describe the Hall effect, e.g., temperature-dependent charge carrier density,⁴ magnetic skew scattering,^{5,6} Anderson's Luttinger-liquid model,^{7,8} and a model based on paired bipolarons.⁹ A phenomenological narrow band model of the electronic band structure of high- T_c superconductors has also been introduced,¹⁰ which in addition to studies of electronic transport properties, also has been used to describe the magnetic susceptibility and the metal insulator transition.^{10,13} It has been shown that the band widths in this model depend on the hole concentration.^{13,18} When the hole concentration is decreased by oxygen reduction¹³ and by substitution of La onto the Ba sites in Y-123,¹⁸ the band width parameters change in the opposite direction.¹⁵

In this paper, the Hall coefficient, R_H , has been measured as a function of temperature and doping concentration in $\text{NdBa}_{2-x}\text{La}_x\text{Cu}_3\text{O}_{7-\delta}$ with $0 \leq x \leq 0.3$. Experimental details are given in Sec. 2. In Sec. 3, the results are described and analyzed in the two different models. The results show that the hole concentration decreased with increased La doping concentration. Comparison between the phenomenological narrow band model and the Anderson model suggests that the holes were localized by La doping. The results are briefly summarized in Sec. 4.

2. Experimental Method

Polycrystalline samples with the composition $\text{NdBa}_{2-x}\text{La}_x\text{Cu}_3\text{O}_{7-\delta}$ ($0 \leq x \leq 0.3$) were prepared by a standard solid state powder processing technique, the details of which are given in Ref. 19. High purity powders of Nd_2O_3 , BaCO_3 , CuO and La_2O_3 were first dried and then mixed in the required proportions and ground. The samples were pressed into pellets and calcined in air at 900, 920, and 920°C with intermediate grindings. Finally, the samples were annealed in flowing oxygen at 460°C for three days and the temperature was decreased to room temperature at the rate of 12°C/h.

X-ray diffraction (XRD) analysis was used to characterize the samples. The XRD results for these samples showed that all samples had a single-phase orthorhombic 123 structure.

Resistivity and Hall voltage measurements were made on sintered bars with typical dimensions $0.5 \times 2.5 \times 6 \text{ mm}^3$. Electrical leads were attached to the sample

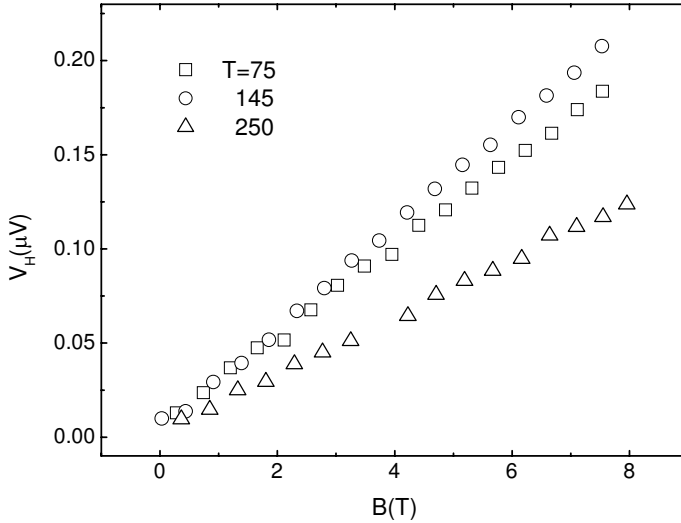


Fig. 1. The Hall voltage versus magnetic field and temperature for $x = 0.15$.

by silver paint and heat-treated at 300°C in flowing oxygen for half an hour, which gave contact resistances on the order of $1\text{--}2\ \Omega$. Measurements were made using standard techniques, with four contacts for longitudinal current and voltage measurements, and additional contacts for transverse voltage measurements, including a potentiometer to compensate for any contact misalignments by nulling this voltage in zero field. The Hall voltage and resistivity were measured simultaneously at each stabilized temperature by sweeping the magnetic field B in steps of $0.5\ \text{T}$ in the sequence $0 \rightarrow +8T \rightarrow 0 \rightarrow -8T \rightarrow 0$. The thermoelectric power was reduced in voltage measurements by switching current polarities. To enhance temperature stability, the samples and a thermometer were placed in a vacuum shield, with a weak thermal link to the surroundings. The temperature error during field sweeps was at most $0.5\ \text{K}$. Hall voltage measurements were made with a dc picovoltmeter with a resolution of $100\text{--}300\ \text{pV}$. The Hall voltage versus B was linear for all samples at temperatures above T_c . The results are shown in Fig. 1 for $x = 0.15$ and $T = 70$, 145 , and $250\ \text{K}$. The Hall coefficient, R_H , was calculated at each temperature from the slope of the straight lines from -8 to $+8\ T$ (calculated as $R_H = V_H d / IB$, where I is current, d is sample width, and B is magnetic field).

3. Results and Discussion

Figure 2 shows R_H as a function of temperature and La doping for $\text{NdBa}_{2-x}\text{La}_x\text{Cu}_3\text{O}_{7-\delta}$ ($0 \leq x \leq 0.3$). R_H is positive in the normal state for all samples, which shows that the charge carriers are holes. This figure also shows that R_H increases with increasing temperature, has a maximum close to T_c for all samples, and after that has a temperature dependence of approximately $1/T$ up

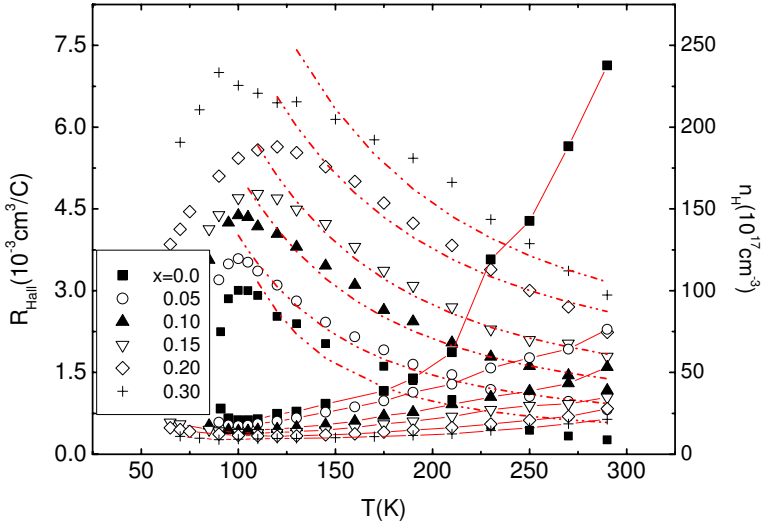


Fig. 2. The temperature dependence of the Hall coefficient (R_H) and Hall concentration (n_H) as a function of doping concentration. The dot curves show n_H . The dash-dot curves are fits to Eq. (1).

to room temperature such as the high temperature, which is typical for superconductor compounds.^{20,22} The temperature dependence of R_H at low temperatures is stronger than that at higher temperatures. The Hall coefficient increases with increasing La doping concentration for all samples and over the whole temperature range from T_c up to room temperature. Since the charge carriers are holes, the increasing R_H shows that substitution of La^{+3} onto Ba^{+2} sites adds electrons into the structure. In Fig. 2, we have also presented the Hall concentration (calculated as $n_H = 1/R_H$) plotted as a function of temperature and La doping concentration. As can be seen, n_H decreases with increasing La doping concentration.

The Hall coefficient in the normal state was analyzed within both the phenomenological narrow band model¹³ and the Anderson model.⁸

3.1. Phenomenological narrow band model

In the phenomenological narrow band model,¹³ it was found that all the features of the resistivity, $\rho(T)$, the thermoelectric power, $S(T)$, and the Hall coefficient, $R_H(T)$, for the Y-123 system in the normal state could be explained. These transport properties were described quantitatively on the basis of a band model that assumed the existence of a narrow peak in the electronic density of states, $D(E)$, close to the Fermi level. This model contains three main parameters for $\rho(T)$ and $S(T)$, and an additional one for $R_H(T)$: (i) the band filling by electrons, $F = n/N$, where n is the electron density and N is the total number of states in the band, (ii) the total effective band width, w_D , in $D(E)$. (iii) The conductivity effective band width, w_σ , in the longitudinal conductivity, $\sigma(E)$, and (iv) for R_H , the transverse

effective band width, $w_{\sigma H}$, in the transverse conductivity, $\sigma_H(E)$. Using rectangular approximations for $D(E)$, $\sigma(E)$, and $\sigma_H(E)$, the results for $R_H(T)$ can be written as:

$$R_H = \frac{\langle \sigma_H \rangle}{\langle \sigma \rangle^2} \frac{(z-1)(v-1)^2(1+zu)^2(z+u)^2}{z(1+z)(z+v)(1+zv)(u^2-1)^2}, \tag{1}$$

$$\mu^* = \frac{\mu}{k_B T} = \ln \frac{\sinh\left(\frac{F w_D}{2k_B T}\right)}{\sinh\left(\frac{(1-F)w_D}{2k_B T}\right)} \tag{2}$$

where $w_D^* = w_D/2k_B T$, $w_\sigma^* = w_\sigma/2k_B T$, $w_{\sigma H}^* = w_{\sigma H}/2k_B T$, $z = \exp(\mu^*)$, $v = \exp(w_{\sigma H}^*)$, $u = \exp(w_\sigma^*)$. μ is the electron chemical potential and k_B is the Boltzmann constant. $\langle \sigma \rangle$ and $\langle \sigma_H \rangle$ are the averages of the longitudinal and transverse (Hall) conductivity in the intervals w_σ and $w_{\sigma H}$, respectively.

We have fitted the $R_H(T)$ data to Eq. (1), as shown by the dotted curves in Fig. 2, and estimated the band parameters. The relative band widths ($w(x)/w(0)$) are shown in Fig. 3. All band widths (w_D , w_σ , $w_{\sigma H}$) increase with increasing doping concentration, x . An increase in all band width values is in agreement with decreasing hole concentration.

Figure 4 shows the variations of the filling factor, $F = n/N$, with doping concentration. As can be seen, with increasing doping concentration, F values are slightly increased. The increase in F shows that increasing La doping leads to additional electron and decreasing holes concentration in CuO_2 planes.

The tendency for Anderson localization at the band edges can be conveniently described by the parameter $c = w_D/w_\sigma$.¹³ For $\text{NdBa}_{2-x}\text{La}_x\text{Cu}_3\text{O}_{7-\delta}$, the result

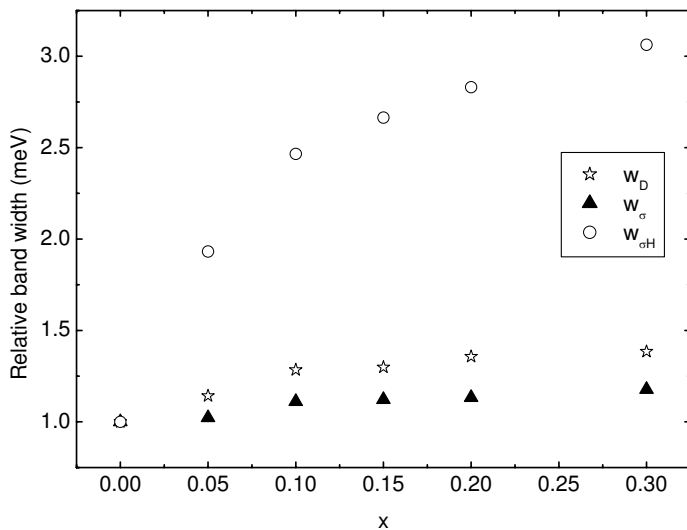


Fig. 3. The relative band widths in the phenomenological narrow band model versus x for $\text{NdBa}_{2-x}\text{La}_x\text{Cu}_3\text{O}_{7-\delta}$.

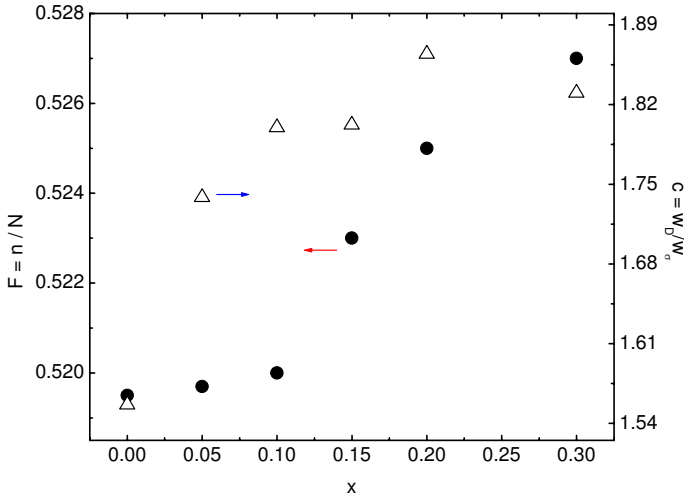


Fig. 4. F (left hand scale) and $c = w_D/w_\sigma$ (right hand scale) versus x for $\text{NdBa}_{2-x}\text{La}_x\text{Cu}_3\text{O}_{7-\delta}$ from the phenomenological narrow band model.

for c are shown in Fig. 4. c increases with doping concentration. These results for c suggest an increasing tendency towards localization and therefore an increase in electronic disorder with increasing doping concentration. Such disorder would arise from the random occupation by La of some Ba sites. We therefore conclude that the increase in R_H and the depression of T_c with doping are due to both charge filling and charge localization on the CuO_2 planes, in addition to increased electronic disorder.

3.2. Anderson model

In the Anderson model,⁸ the conductivity in the longitudinal and transverse directions are governed by two different mechanisms and two different relaxation times, due to spin-charge separation in the CuO_2 planes. The longitudinal (transport) relaxation time follows a linear T^{-1} dependence ($\tau_{\text{tr}} \propto T^{-1}$), and the transverse (Hall) relaxation time, follows an $a \sim T^{-2}$ dependence ($\tau_H \propto T^{-2}$). τ_{tr} gives the well-known linear- T resistivity, ρ , while τ_H gives the temperature dependence of the Hall angle, $\cot \theta_H \propto T^2$. Allowing also for a temperature independent impurity contribution, β , one can write:⁸

$$\cot \theta_H = \rho/R_H B = \alpha T^2 + \beta, \quad (3)$$

where α and β are constants. Chien *et al.*⁷ derived the following relation from Anderson theory:

$$\alpha = \frac{k_B^2 \hbar n}{e B w_s^2}, \quad (4)$$

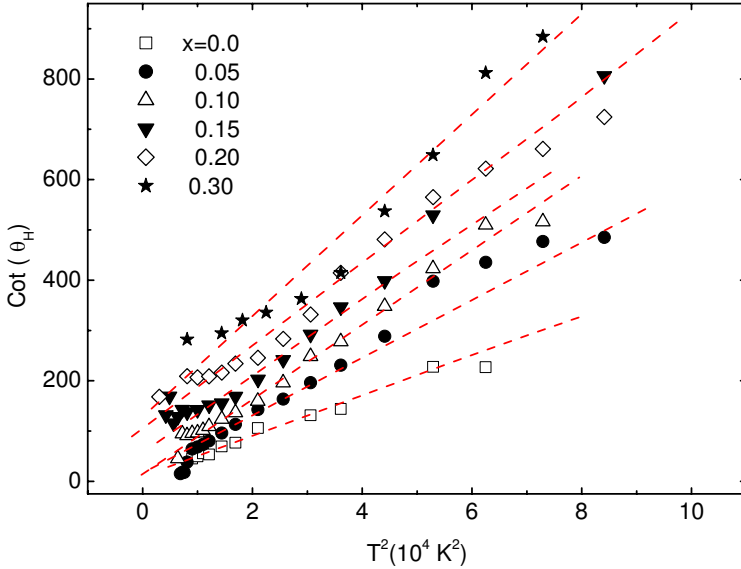


Fig. 5. T^2 dependence of $\cot \theta_H = \rho/R_H B$ in $B = 8 T$ for $\text{NdBa}_{2-x}\text{La}_x\text{Cu}_3\text{O}_{7-\delta}$ as a function of doping concentration x . The dashed lines are fits to Eq. (3).

where $n = k_F^2/2\pi$ is the carrier density, B the applied magnetic field, h is Planck's constant, and w_s the spinon band width, which is proportional to the superexchange J .

It was found in various cuprate superconductors that the results for $\cot \theta_H$ are in broad agreement with Eq. (3). In some cases, deviation from this law was reported at both low and high temperatures.^{6,23} The deviation at low temperature may be caused by the opening of a pseudogap in the density of states,²³ while the origin of the anomaly at high temperatures is not clear.

Figure 5 shows $\cot \theta_H$ versus T^2 in a magnetic field, $B = 8 T$. The data were calculated from the results for $\rho(T)$ and $R_H(T)$. Irrespective of the complicated temperature dependencies of ρ ²⁴ and R_H (Fig. 2), a quadratic-like temperature dependence of $\cot \theta_H$ is obtained for all x values. A slight deviation from a T^2 dependence was observed at both low and high temperatures. α and β were determined from Fig. 5 and using Eq. (3). The doping dependences of α and β are shown in Fig. 6.

It can be seen that both β and α increase with increasing La doping concentration. The increased β can be ascribed to increased disorder in the CuO_2 planes.^{7,12} These results are in agreement with the obtained results for $\text{Nd}_{1-2x}\text{Ca}_x\text{M}_x\text{Ba}_2\text{Cu}_3\text{O}_{7-\delta}$ (with $M = \text{Th}, \text{Pr}$),²⁵ $\text{Y}_{1-x}\text{Ca}_x\text{Ba}_2\text{Cu}_3\text{O}_{7-\delta}$ thin films,²⁶ $\text{YBa}_2\text{Cu}_{3-x}\text{Zn}_x\text{O}_{7-\delta}$ single-crystals,⁷ and $\text{Nd}_{1-x}\text{Ca}_x\text{Ba}_2\text{Cu}_3\text{O}_{7-\delta}$.²⁷ The increase in α may correspond to variations in the spinon band width, w_s , and in n [see Eq. (4)].

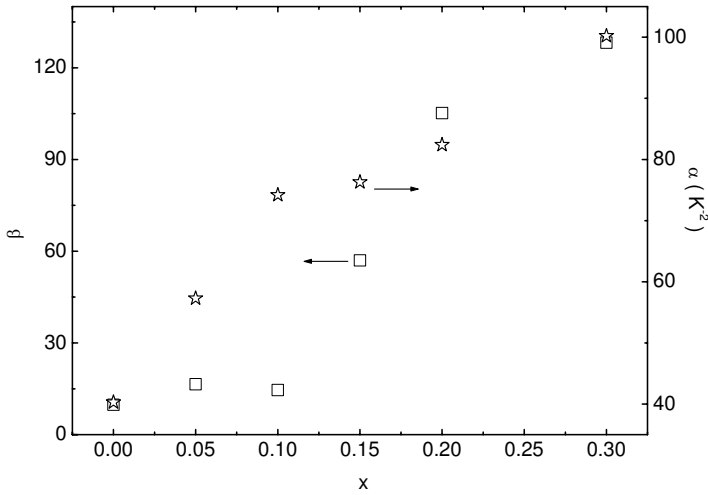


Fig. 6. Doping dependence of β and α in Eq. (3) for $\text{NdBa}_{2-x}\text{La}_x\text{Cu}_3\text{O}_{7-\delta}$.

3.3. Comparison between models

The two different models used to analyze $R_H(x, T)$ are based on different assumptions and are therefore in general difficult to compare quantitatively. However, as mentioned above, β in the Anderson model and the parameter $c = w_D/w_\sigma$ in the phenomenological narrow band model both depend on disorder. It can be seen that both β and c decrease with increasing T_c . Therefore, these results for both β and c suggest a tendency towards carrier localization with decreasing T_c . This

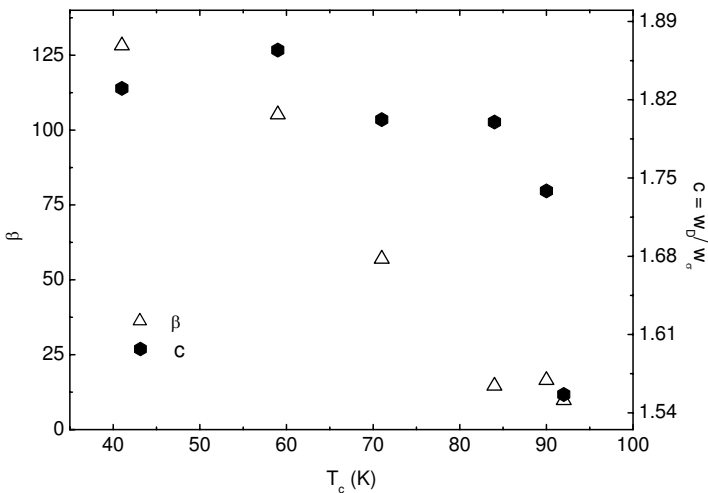


Fig. 7. $c = w_D/w_\sigma$ versus critical temperature T_c from the phenomenological narrow band model (right hand scale). β as a function of T_c from the Anderson model (left hand scale). Data for T_c have been obtained from Ref. 24.

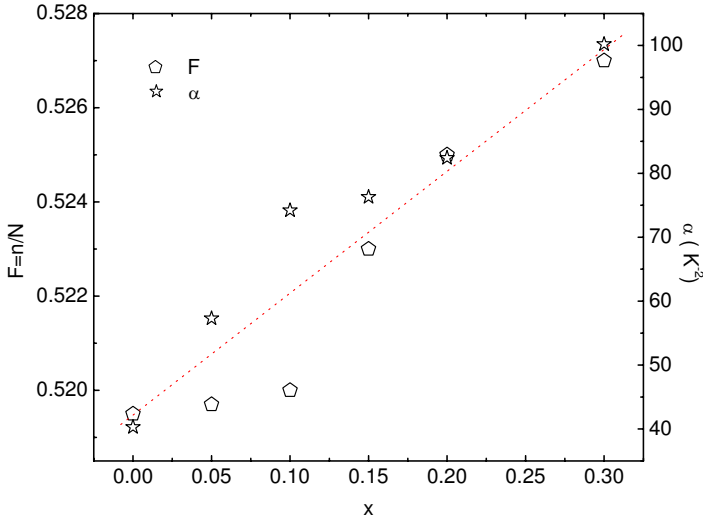


Fig. 8. Band filling by electrons F in the phenomenological narrow band model (left hand scale) and α in the Anderson model (right hand scale) versus La doping concentration for $\text{NdBa}_{2-x}\text{La}_x\text{Cu}_3\text{O}_{7-\delta}$.

charge carrier localization can be one of the main reasons for the decreasing hole concentration in the CuO_2 planes.

The band filling factor F in the phenomenological narrow band model corresponds qualitatively to the α parameter in the Anderson model. According to the definition of F and Eq. (4), both parameters depend on charge carrier density. The results for comparison are shown in Fig. 8. There is good agreement between both parameters, which suggest a decreased hole concentration with increased doping concentration.

4. Brief Conclusion

The Hall effect behaviour of sintered samples of $\text{NdBa}_{2-x}\text{La}_x\text{Cu}_3\text{O}_{7-\delta}$ (with $0 \leq x \leq 0.3$) was studied in the normal state. The Hall coefficient increases with increasing La concentration. The phenomenological narrow band and the Anderson models could well-describe the results for the Hall coefficient. On the basis of the phenomenological narrow band model, as La doping concentration increased, the conduction band increases and the degree of band filling with electrons also increases. In the Anderson model, the temperature dependent part of the Hall angle is roughly proportional to T^2 and independent of the hole concentration and disorder. The results of both models indicated that La had introduced electronic disorder, which drives a tendency towards the localization of mobile holes in the CuO_2 planes. Therefore, in addition to hole filling by La, hole localization could be another reason for the decreasing superconductivity critical temperature.

References

1. H. Kontani *et al.*, *Phys. Rev. B* **59**, 14723 (1999).
2. M. Akhavan, *Physica B* **321**, 265 (2002).
3. H. Fjellvåg *et al.*, *Physica C* **162**, 49 (1989).
4. Y. Kubo, T. Kondo, Y. Shimakawa, T. Manako and H. Igarashi, *Phys. Rev. B* **45**, 5553 (1992).
5. A. T. Fiory and G. S. Grader, *Phys. Rev. B* **38**, 9198 (1988).
6. B. Wuyts, V. V. Moshchalkov and Y. Bruynseraede, *Phys. Rev. B* **53**, 9418 (1996).
7. T. R. Chien, Z. Z. Wang and N. P. Ong, *Phys. Rev. Lett.* **67**, 2088 (1991).
8. P. W. Anderson, *Phys. Rev. Lett.* **67**, 2092 (1991).
9. A. S. Alexandrov, V. N. Zavaritsky and S. Dzhumanov, *Phys. Rev. B* **69**, 052505 (2004).
10. V. V. Moshchalkov, *Physica C* **156**, 473 (1988).
11. V. V. Moshchalkov, *Physica B* **163**, 59 (1990).
12. C. Quitmann, D. Andrich, C. Jarchow, M. Fleuster, B. Beschoten, G. Güntherodt, V. V. Moshchalkov, G. Mante and R. Manzke, *Phys. Rev. B* **46**, 11813 (1992).
13. V. E. Gasumyants, V. I. Kaidanov and E. V. Valadimirskaya, *Physica C* **248**, 255 (1995).
14. V. E. Gasumyants, V. V. Valadimirskaya, M. V. Elizarova and N. V. Ageev, *Phys. Solid State* **40**, 1943 (1993).
15. V. V. Valadimirskaya, V. E. Gasumyants and I. B. Patarina, *Phys. Solid State* **37**, 1084 (1995).
16. V. E. Gasumyants, M. V. Elizarova and I. B. Patarina, *Supercond. Sci. Technol.* **13**, 1600 (2000).
17. N. V. Ageev, V. E. Gasumyants and V. I. Kaidanov, *Phys. Solid State* **37**, 1171 (1995).
18. V. E. Gasumyants, E. V. Valadimirskaya and I. B. Patarina, *Phys. Solid State* **40**, 14 (1998).
19. S. R. Ghorbani, M. Andersson and Ö. Rapp, *Phys. Rev. B* **66**, 104519 (2002).
20. J. M. Harris, H. Wu, N. P. Ong, R. L. Meng and C. W. Chu, *Phys. Rev. B* **50**, 3246 (1994).
21. P. S. Wang, J. C. Williams, K. D. Rathnayaka, B. D. Hennings and D. G. Naugle, *Phys. Rev. B* **47**, 1119 (1993).
22. R. Jin and H. R. Ott, *Phys. Rev. B* **57**, 13872 (1998).
23. Y. Abe, K. Segawa and Y. Ando, *Phys. Rev. B* **60**, R15055 (1999).
24. S. R. Ghorbani, *Iranian J. Phys. Res.* **6**, 147 (2007).
25. S. R. Ghorbani, M. Anderson and Ö. Rapp, *Physica C* **424**, 159 (2005).
26. H. Yakabe, I. Terasaki, M. Kosuge, Y. Shiohara and N. Koshizuka, *Phys. Rev. B* **54**, 14986 (1996).
27. S. R. Ghorbani, M. Anderson and Ö. Rapp, *Physica C* **390**, 161 (2003).